Vibrational Spectroscopy in Biology

Dr. Vassilis Papadakis

BioNDT Lab

Foundation for Research and Technology – Hellas
Institute of Molecular Biology and Biotechnology
Heraklion Crete, Greece

Vassilis_Papadakis@imbb.forth.gr
www.biondt.gr

FORTH

ΙΣΝ/SNF ΙΔΡΥΜΑ ΣΤΑΥΡΟΣ ΝΙΑΡΧΟΣ STAVROS NIARCHOS FOUNDATION

Theory

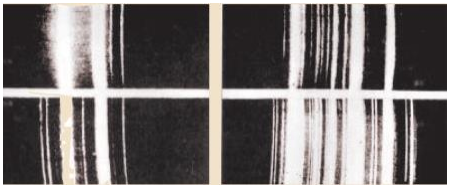

Interaction of radiation and matter

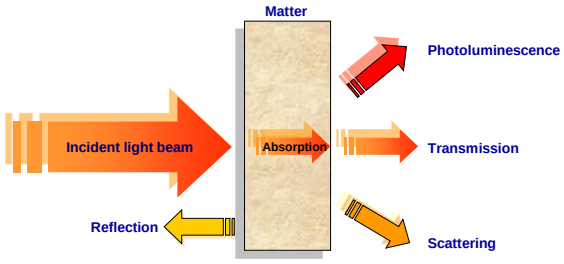

$$\nu = \frac{1}{2\pi}\sqrt{\frac{k}{\mu}}$$

$$\mu = \frac{m_1 \cdot m_2}{m_1 + m_2}$$ reduced mass.

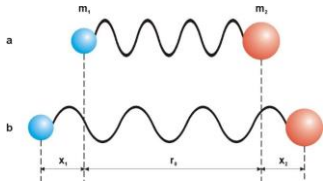

Mechanical model of a vibrating diatomic molecule

Photo-Molecular Interactions

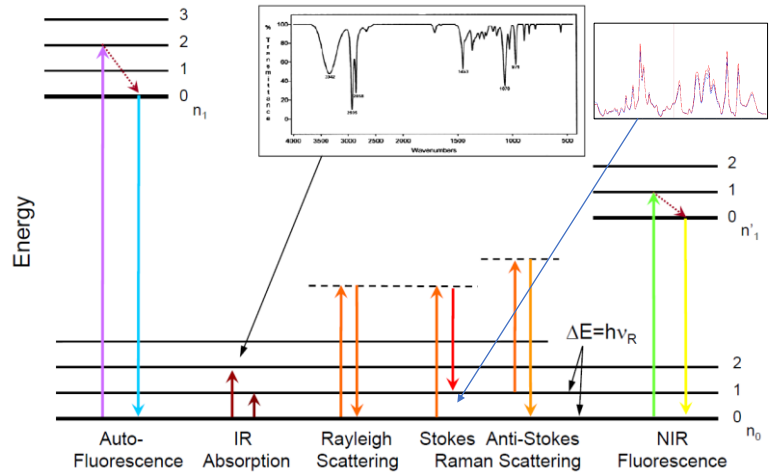

Vibrational spectroscopy - the main principle

Extension from r_0 **(equilibrium distance)**
- **absorption** of energy **E**
- relaxation to r_0
- Potential energy **V**
- **Vibration**

Hooke's law

$F = -k\,x$

$V = \int -F\,dx = \int kx\,dx$

$V = \frac{1}{2} k\,x^2$

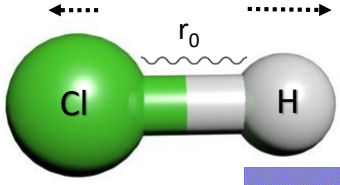

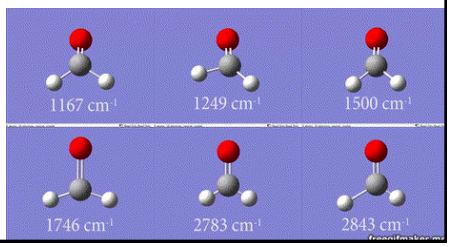

- Each **vibrational mode** of a molecule is characterized by a different **spectral signature**!

FT-IR

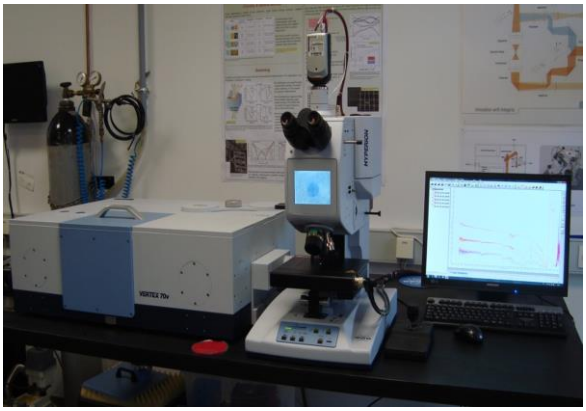

Fourier Transform Infra Red (FT-IR)

- An Infrared spectrum is a ***fingerprint***
- Absorption peaks correspond to ***frequencies*** of bond vibrations
- Each different material is a **unique** combination of atoms

IR results in a unique identification of every different kind of material!

FingerPrint

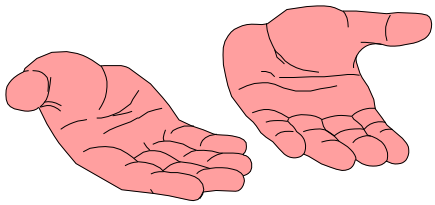

Infrared Spectroscopy

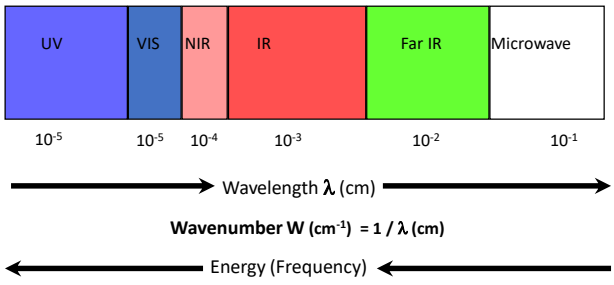

Light, or more properly, *electromagnetic radiation,* can be described in terms of frequency ν or wavelength λ .

Energy of radiation increases with increasing frequency and decreases with increasing wavelength

Separation of spectral ranges

Wavenumber scale

>14,000 cm-1	14,000 to 4000 cm-1	4000 to 400 cm-1	400 to 4 cm-1	< 4 cm-1
Visible, UV & X-Rays	**Near Infrared**	**Mid Infrared**	**Far Infrared**	**Microwaves Radio Waves**

HIGHER WAVENUMBER
HIGHER FREQUENCY
HIGHER ENERGY
SHORTER WAVELENGTH

LOWER WAVENUMBER
LOWER FREQUENCY
LOWER ENERGY
LONGER WAVELENGTH

Vibration theory

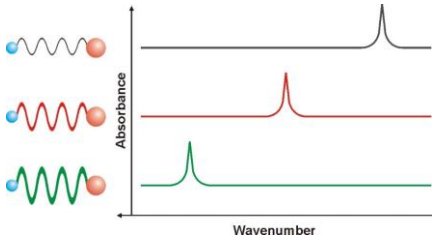

3 absorption peaks for different force constants. Note that by convention, in infrared spectroscopy wavenumbers are plotted right-to-left; i.e. highest wavenumber to the left.

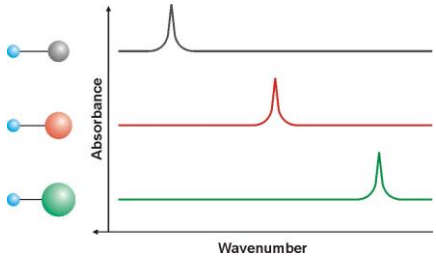

3 absorption peaks for different atomic masses. Note that by convention, in infrared spectroscopy wavenumbers are plotted right-to-left; i.e. highest wavenumber to the left.

FT-IR spectrometer layout

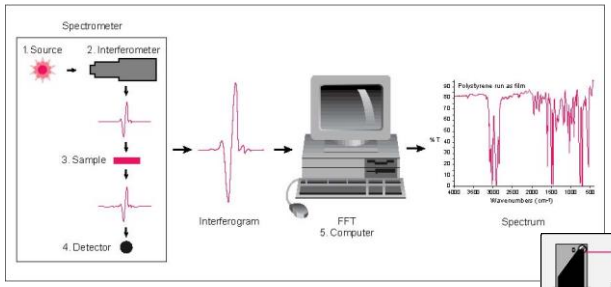

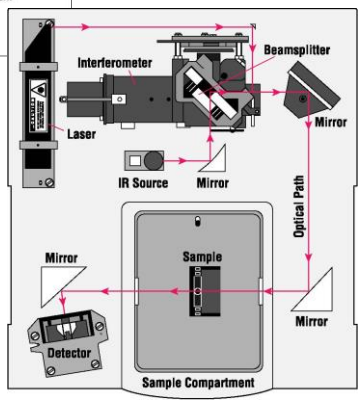

Fourier Transformation

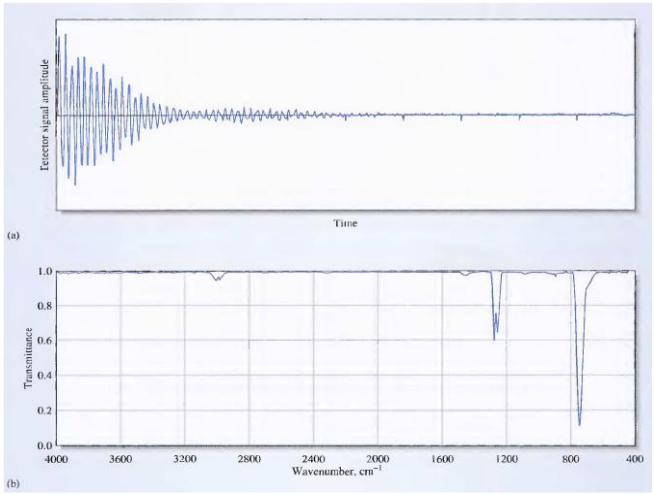

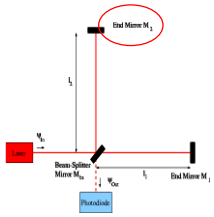

Advantages of FTIR (technique)

- Established technology
- Universal technique
- sensitivity 10^{-6} grams
- fast and easy
- relatively inexpensive measurement
- rich information signals
- sensitive to “molecules”-anything that contains chemical bonds
- vast majority of molecules in the universe absorb mid-infrared light, making it a highly useful tool

Heteronuclear diatomic molecule

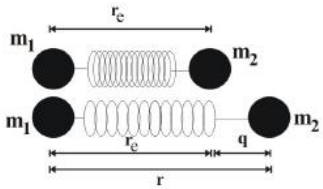

Disadvantages of FTIR

- *Cannot detect atoms or monoatomic ions*
  - single atomic entities contain no chemical bonds
- *Cannot detect molecules comprised of two identical atomS symmetric*
  - such as N_2 or O_2.
- *Aqueous solutions are very difficult to analyze*
  - water is a strong IR absorber
- *Complex mixtures*
  - samples increase complexity to already complex spectra
- *Point of measurement*
  - ATR → 1-2 mm
  - MicroATR → ~ 50 um

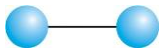

Homonuclear diatomic molecule

Reference library structure

1.) Measure reference sample → **2.) Calculate average spectrum & threshold values** → **3.) Library structure & validation**

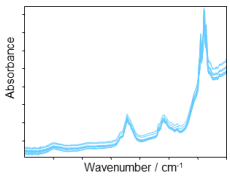

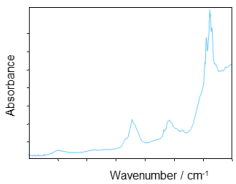

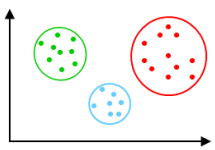

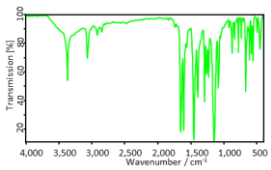

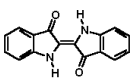

Examples

Published in final edited form as:
Nat Protoc. 2014 August ; 9(8): 1771–1791. doi:10.1038/nprot.2014.110.

Using Fourier transform IR spectroscopy to analyze biological materials

Matthew J Baker[1,13], **Júlio Trevisan**[2,3], **Paul Bassan**[4], **Rohit Bhargava**[5], **Holly J Butler**[2], **Konrad M Dorling**[1], **Peter R Fielden**[6], **Simon W Fogarty**[2,7], **Nigel J Fullwood**[7], **Kelly A Heys**[2], **Caryn Hughes**[4], **Peter Lasch**[8], **Pierre L Martin-Hirsch**[2], **Blessing Obinaju**[2], **Ganesh D Sockalingum**[9], **Josep Sulé-Suso**[10], **Rebecca J Strong**[2], **Michael J Walsh**[11], **Bayden R Wood**[12], **Peter Gardner**[4], and **Francis L Martin**[2]

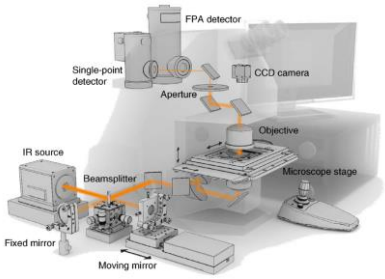

Description of a protocol for collecting IR spectra and images from biological samples (e.g., fixed cytology and tissue sections, live cells or biofluids)
Assesses the instrumental options available, appropriate sample preparation, different sampling modes as well as recent advances in spectral data acquisition.

Examples

HHS Public Access
Author manuscript
Nat Protoc. Author manuscript; available in PMC 2015 August 01.

Published in final edited form as:
Nat Protoc. 2014 August ; 9(8): 1771–1791. doi:10.1038/nprot.2014.110.

Using Fourier transform IR spectroscopy to analyze biological materials

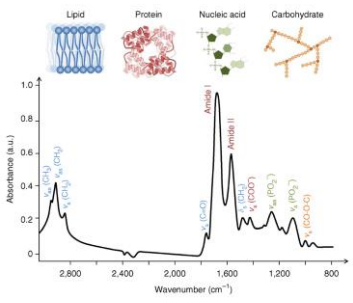

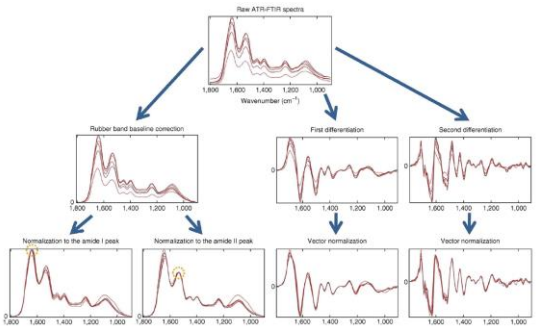

Examples

J. Biophotonics 1–11 (2016) / DOI 10.1002/jbio.201600173

Journal of BIOPHOTONICS

FULL ARTICLE

Distinction between breast cancer cell subtypes using third harmonic generation microscopy

Evangelia Gavgiotaki[1, 2], George Filippidis[*, 1], Haris Markomanolaki[2], George Kenanakis[1], Sofia Agelaki[2], Vassilis Georgoulias[2], and Irene Athanassakis*[*, 3]*

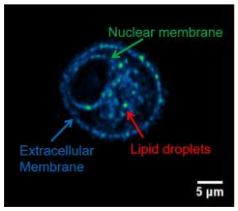

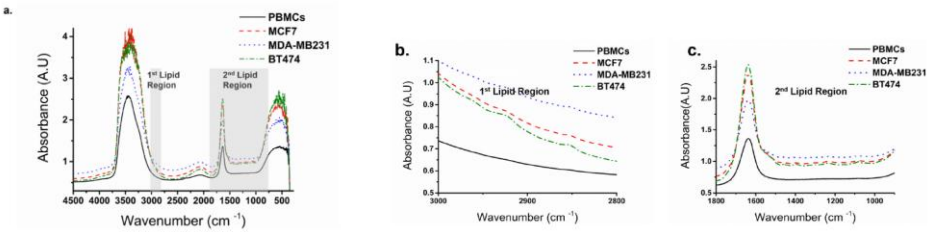

FTIR spectra of cancer cell lines and control cells (PBMCs) and their lipid regions (b) 2800–3000 cm^{-1} and (c) 900–1800 cm^{-1} respectively.

Examples

J. Biophotonics 1–11 (2016) / DOI 10.1002/jbio.201600173

Journal of BIOPHOTONICS

FULL ARTICLE

Distinction between breast cancer cell subtypes using third harmonic generation microscopy

Evangelia Gavgiotaki[1, 2], George Filippidis[*, 1], Haris Markomanolaki[2], George Kenanakis[1], Sofia Agelaki[2], Vassilis Georgoulias[2], and Irene Athanassakis*[*, 3]*

The absorption wavelengths correspond to cholesterol, phospholipids and C=O stretching modes mostly define lipid rafts [1].
1737 cm^{-1} (lipids) [2, 3],
1746 cm^{-1} (lipids) [4],
2845 cm^{-1} (lipids, cholesterol/phospholipids) [5, 6],
2853–2858 cm^{-1} (lipids) [5, 7] and
2910 cm^{-1} (cholesterol/phospholipids) [6],

[1] Z. Arsov, L. Quaroni *Biochimica et Biophysica Acta (BBA) - Biomembranes*. **2008**, 1778, 880-889.
[2] H. Fabian, M. Jackson, L. Murphy, P. H. Watson, I. Fichtner, H. H. Mantsch *Biospectroscopy*. **1995**, 1, 37-45.
[3] S. Yoshida, M. Miyazaki, K. Sakai, M. Takeshita, S. Yuasa, A. Sato, T. Kobayashi, S. Watanabe, H. Okuyama *Biospectroscopy*. **1997**, 3, 281-290.
[4] G. Shetty, C. Kendall, N. Shepherd, N. Stone, H. Barr *British Journal of Cancer*. **2006**, 94, 1460-1464.
[5] G. I. Dovbeshko, N. Y. Gridina, E. B. Kruglova, O. P. Pashchuk, Talanta. 2000, 53, 233-246
[6] M. Huleihel, A. Salman, V. Erukhimovitch, J. Ramesh, Z. Hammody, S. Mordechai *Journal of Biochemical and Biophysical Methods*. **2002**, 50, 111-121.
[7] M. F. K. Fung, M. K. Senterman, N. Z. Mikhael, S. Lacelle, P. T. T. Wong *Biospectroscopy*. **1996**, 2, 155-165.

RAMAN

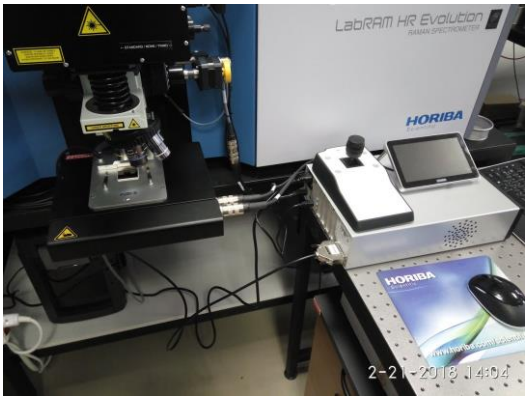

Infrared absorption

IR and Raman are complementary techniques

- Symmetric molecules with a center of inversion have vibrations which are either Raman or IR active, but not both (e.g. benzene)
- Molecules with no symmetry are active in both methods

(N)IR absorption	Raman
Absorption	Scattering
Requires change in dipole moment (No symmetric stretches observed, No diatomic activity)	Requires a change in polarizability with vibrational motion
Only observed in NIR and IR spectral regions	Occurs at all wavelengths
Strong signal	Weak signal
High water absorption	Water not a problem
Broad spectral features	Sharp spectral features for molecular fingerprinting
Requires some sample preparation in most cases	Does not require sample preparation

Sir Chandrasekhara Venkata Raman

- Born on 7 November 1888 - 1970
- 1928: He discovered that when light traverses a transparent material, a small percentage of the deflected light changes wavelength
- **1930: Won the Nobel Prize for Physics**
- 1932: He discovered the quantum photon spin, which further confirmed the quantum nature of light

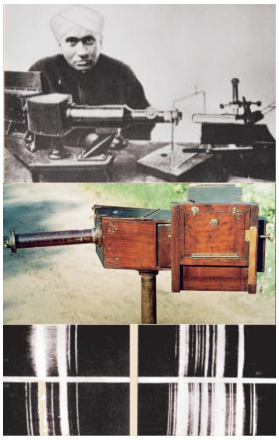

"*The Raman Effect*" commemorative booklet produced by the National Historic Chemical Landmarks program of the American Chemical Society in 1998
(https://www.acs.org/content/acs/en/education/whatischemistry/landmarks/ramaneffect.html)

Basic principles

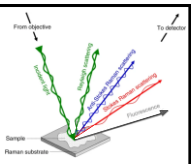

Nature Protocols

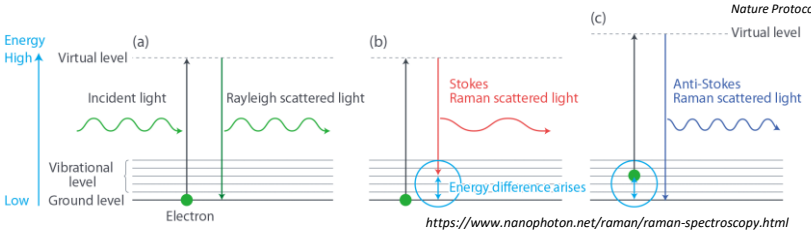

https://www.nanophoton.net/raman/raman-spectroscopy.html

- It relies on **inelastic scattering** of monochromatic (laser) light.
- Raman signal intensity is approximately 10^{-6} of the **Rayleigh** scattered light (elastic scattering)
- **Fluorescence** is much stronger (10^4) than Raman signal.

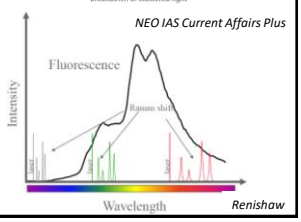

NEO IAS Current Affairs Plus

Renishaw

* Why are we talking about Raman today almost **100 years** later?

Instrumentation

Raman setup (Horiba LabRAM HR)

George Kenanakis

Instrumentation
Horiba LabRAM HR (located at Kenanakis lab – IESL)
Multiple objective lenses (x4, x10, x20, x50, x100)
CLSM

Optimizations/modifications
- 532 nm, 785 nm laser sources
- 9 high refl. mirrors
- Obj. lens x60 NA:1.2 W
- Temperature control stage
- XYZ scanner for mapping
- Koehler illuminator (LED)

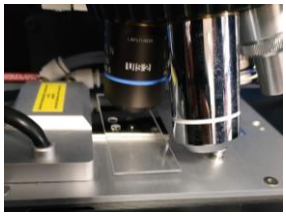

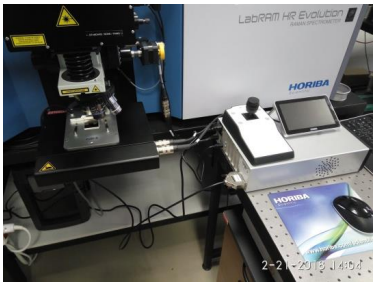

Laser λ (nm)	532	532	532	532	785	785	785	785
Objective lens type		LMPlanFL N	UPLSAPO60XW/1.2			LMPlanFL N	UPLSAPO60XW/1.2	
objective lens magnification	X10	X50	X60	X100	X10	X50	X60	X100
Numerical aperture	0.25	0.5	1.2	0.9	0.25	0.5	1.2	0.9
Spot size (um)	2.596	1.298	0.541	0.721	3.831	1.915	0.798	1.064
Axial resolution (um)	3.494	1.598	0.468	0.685	5.156	2.359	0.691	1.010
Working Distance (mm)		21	0.2			21	0.2	

Raman setup (Renishaw)

- Renishaw Biological Analyzer
- Single laser source at 785 nm
- Fixed obj. lens x50 NA:0.5 LWD
- **Line scan** (70 points, 3750 points/hour)

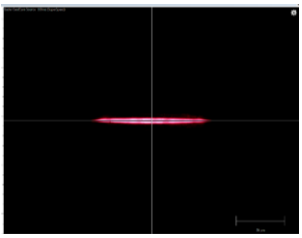

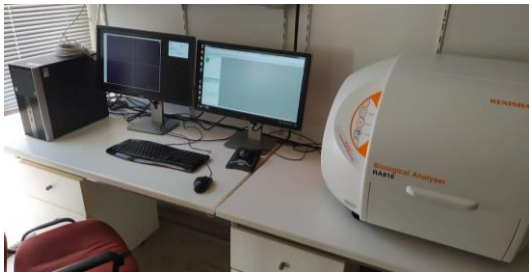

✓Tissue mapping
✓Multi-area acquisition

Raman Signals

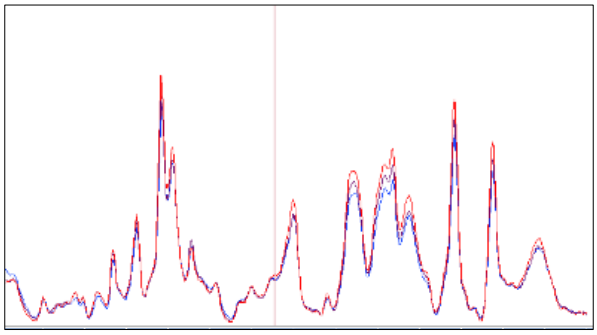

Generic Raman Spectrum

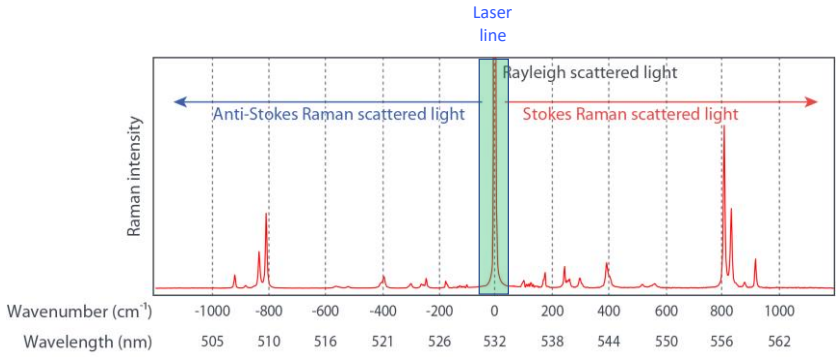

https://www.nanophoton.net/raman/raman-spectroscopy.html

What information can we get?

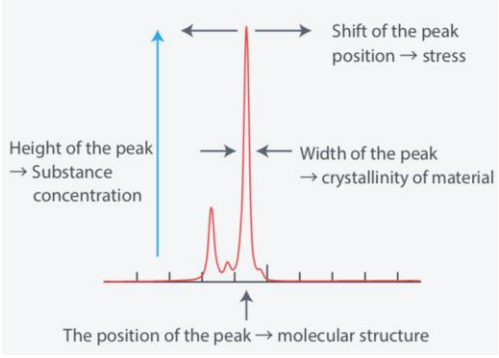

- Raman spectrum provides a **fingerprint** which represents the set of bonds present in a material. **Specific chemical bonds are characterized by the respective vibrational frequencies**
- Vibrational frequencies are sensitive to details of the **structure** and local **environment** of a molecule (symmetry, crystal phase, solvents, interactions etc)
- Relative intensities correspond principally to the bond species **concentration** but it can also be related to the **orientation** of the material or molecule (depends on the incoming laser polarization)

https://www.nanophoton.net/raman/raman-spectroscopy.html

Raman spectrum of a cell nucleus

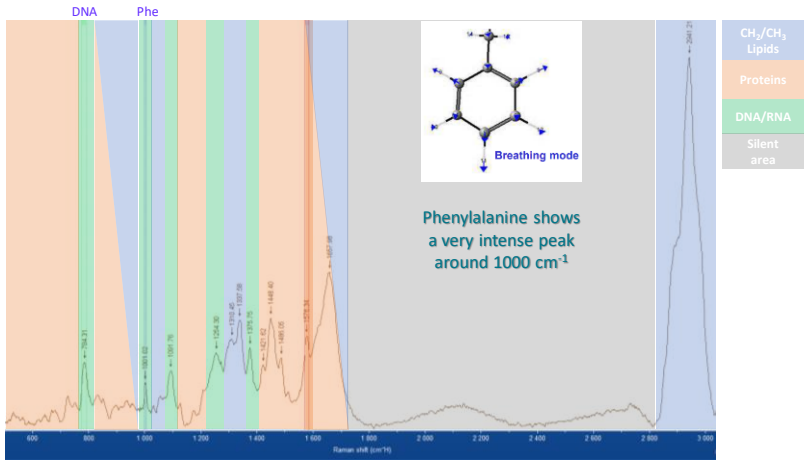

- The major spectral bands are proteins, lipids and nucleic acids
- The band between 400 cm^{-1} and 1800 cm^{-1} is called the **fingerprint region**
- The band between 2800 cm^{-1} and 3050 cm^{-1} corresponds to methylation and lipids

Movasaghi et al, Raman Spectroscopy of Biological Tissues, (2007), Applied Spectroscopy Reviews, 42:5, 493-541

Example of a biological Raman shift

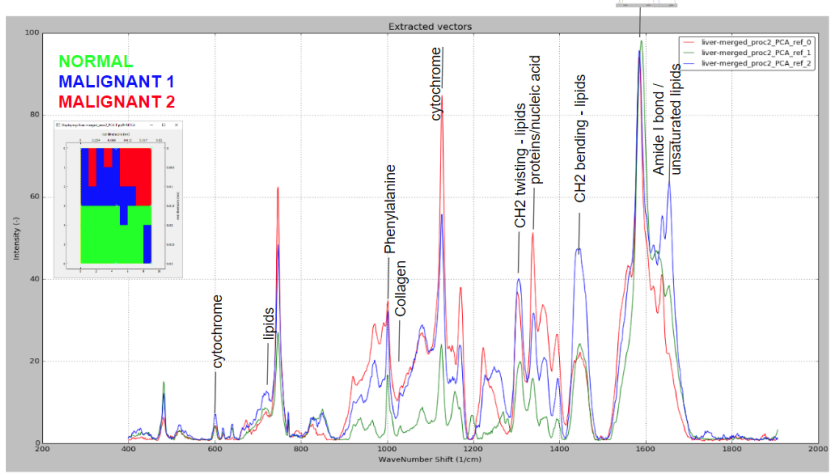

Advantages of Raman spectroscopy for biological research

- ✓Analytical technique with fingerprint signal
- ✓Provides information on chemical phase and bonding
- ✓No size limitations
- ✓Non-destructive, non-invasive
- ✓Resolution capacity: spatial <300nm, axial: <600nm
- ✓ Fast acquisition (0.1 – 60 sec/point scan)
- ✓Can provide chemical image maps
- ✓Label-free

Sample preparation

- No fixation required, label-free

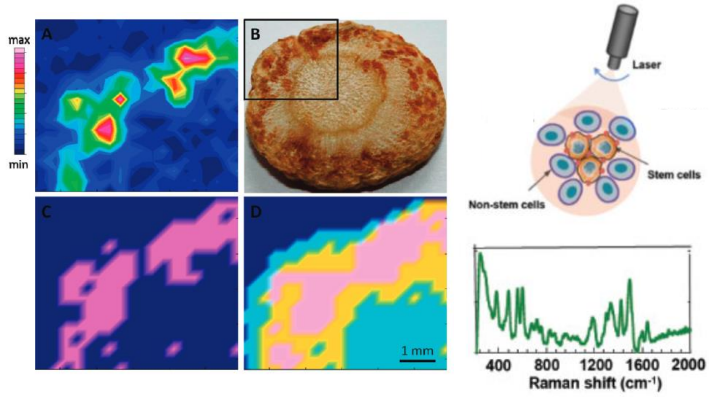

- Drop casting on Raman grade solid substrates (CaF_2, Si, metallic mirrors)
- NOT on glass (provides strong fluorescence)

Roman et al. 2011, Han et al. 2016

Raman database libraries

- Biological tissues and Biological molecules
- SERS DNA (mammalian, synthetic, microorganisms, plants)
- Polyamines-polyamides
- Plant cell wall polymers (there is one for FT-IR signals also)
- Other substances such as α-tocopherol

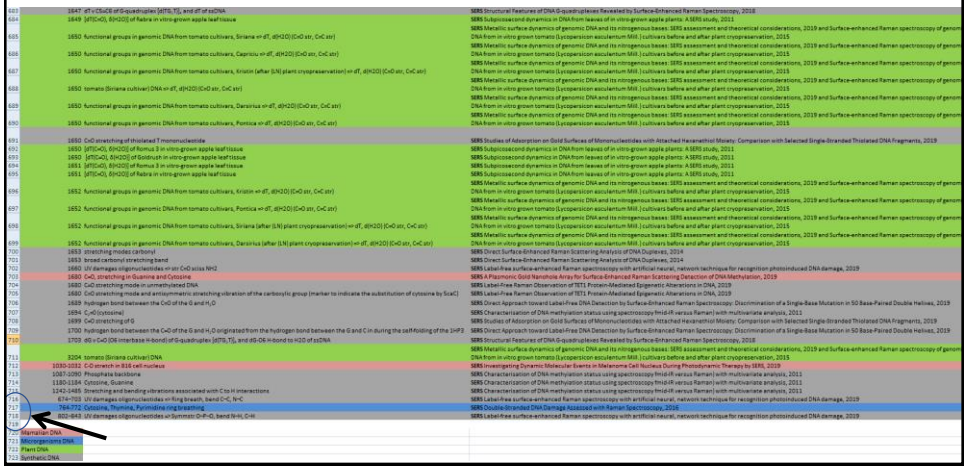

Contribution of vibrational spectroscopy techniques in biological research

- ✓ Detection of compounds of interest in cell, tissue or extracted bio-compound (DNA/RNA)
- ✓ Toxicology/pharmacokinetics
- ✓ In-vivo localization/mapping
- ✓ Concentration evaluation
- ✓ Crystallinity evaluation
- ✓ Epigenetic changes of biomolecules
- ✓ State of biomolecules (phase transition, tension of cell membrane, orientation of microtubules etc)

Relevant research

- RA04 : In vivo Raman Measurements of Human Skin.
- RA05 : SERS analysis of single living lymphocytes.
- RA06 : Raman analysis of single bacteria cells.
- RA07 : Raman mapping of wheat grain kernels.
- RA08 : SERS for Intracellular Imaging.
- RA09 : Insights into thrombosis mechanisms using high resolution SERS.
- RA49 : Raman Analysis of Sperm Nuclear DNA Integrity.
- RA57 : Raman Imaging of monkey brain tissue
- RA59 : Raman investigation of microorganisms on a single cell level.
- RA60 : Investigating the Atherosclerosis Process by Monitoring Lipid Deposits Including Cholesterol and Free Fatty Acids.
- RA62 : Direct identification of clinically relevant microorganisms on solid culture media by Raman spectroscopy

HORIBA

https://www.nature.com/articles/nprot.2016.036

Limitations of Raman spectroscopy

- autofluorescence
- movement of living cells
- databases of reference spectra corresponding to biomolecules under development
- subcellular level localization
- background interfering peaks (sample contaminants, buffer components etc)

Surface Enhanced Raman Scattering (SERS)

Preparation method for SERS

- drop casting of solution (Ag, Au)
- microwave annealing
- thermal processing

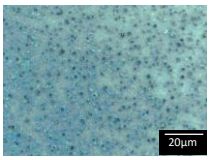

Ag layer on Si (drop casting)

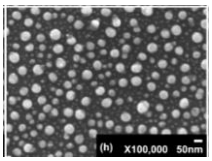

Ag layer on Si (8nm thickness, 10sec MWA)

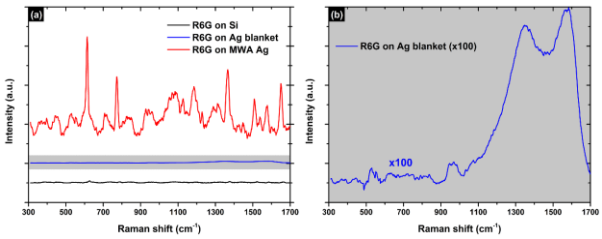

Raman signal enhancement factor: 10^5

Developed for the study of biological samples in small quantities (DNA etc)

Papadakis V., Kenanakis G. Reusable surface enhanced Raman substrates using microwave annealing (2018). APYA

Surface Enhanced Raman Scattering (SERS)

SERS enhancement is dependent on the **interaction** between target molecule and SERS substrate:

→ **size, shape and structure** of substate material

1. **plasmonic** metals (**Au, Ag, Cu**)
2. **bimetallic** (alloyed, core-shell)
3. **anisotropic** (rods, wires)
4. **patterned**
5. **non-traditional** (photonic crystal fibers)

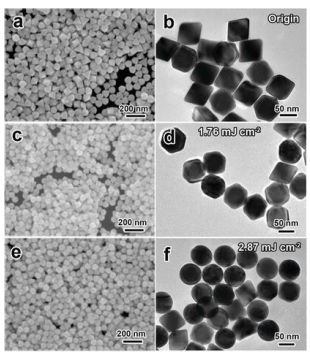

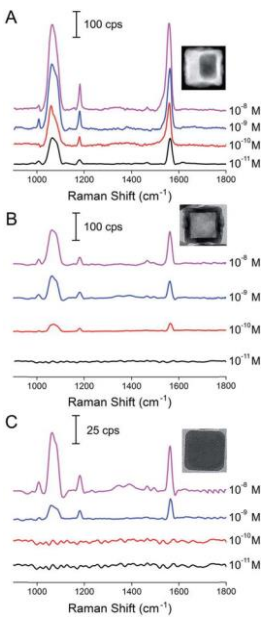

Li et al. Hollow nanocubes made of Ag-Au alloys for SERS detection with sensitivity of 10–8 M for melamine (2014). Journal of Materials Chemistry C.

Liu et al. Rapid synthesis of monodisperse Au nanospheres through a laser irradiation-induced shape conversion, self-assembly and their electromagnetic coupling SERS enhancement (2015). Scientific Reports

Applications and pilot measurements

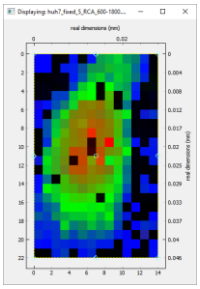

Raman hyperspectral imaging of a fixed cell

DNA

https://www.futurity.org/dna-nanoparticles-metamaterials-1659312/

Vibrational spectroscopy analysis of DNA damage under UV light and repair efficiency by photolyases

DNA was extracted from mice cells expressing a CPD photolyase transgene

a) Untreated cells

b) Cells irradiated with UV light (10J/m^2)

c) Cells irradiated with UV light (10J/m^2) and kept in the dark (1.5h)

d) Cells irradiated with UV light (10J/m2) and placed under visible light (1.5h)

10 μL of DNA (1μg/μL) in pure water left to dry on a CaF_2 microscope slide

Callina Stratigi

Georgia Chatzinikolaou

George Garinis

DNA (mouse) spectral differences due to UV irradiation

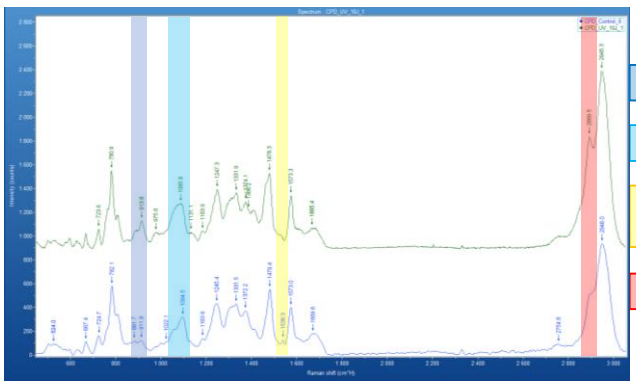

Proteins

PO_2^- stretching (DNA/RNA)

Amide carbonyl group and aromatic hydrogens

CH_3 symmetric stretch

DNA (mouse) spectral differences due to CPD photolyase activity

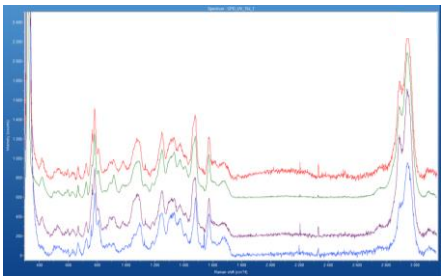

Raman Spectroscopy of DNA

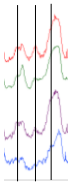

cm-1	Assigned
504	C-OH3 torsion of methoxy group 1
888	889 Methylene rocking / 890 Protein bands structural modes of tumors β-anomers
916	Ribose vibration, distinct RNA mode / 918 proline, hydroxyproline
995	C-O ribose, C-C

SERS Spectroscopy of DNA

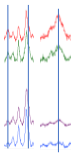

cm-1	Assigned
660	662 C-S stretching mode of cystine (collagen type I)
1052	1053 C-O stretching, C-N stretching (protein) 1055 In the solid, the most significant difference between the two nucleic acids is the ratio intensity of the bands in this area
2878 - 2919	CH2 asymmetric stretch of lipids and proteins

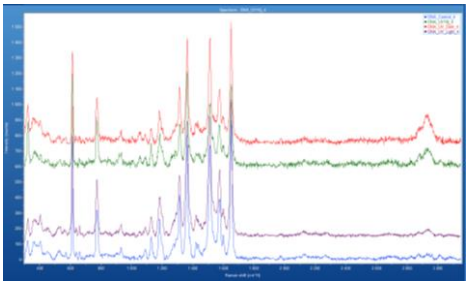

Raman spectroscopy characterization of cell-free DNA methylation

ccfDNA was extracted from human blood

a) Normal Male and Female
b) Diabetic
c) Metastatic Cancer
d) Adjuvant

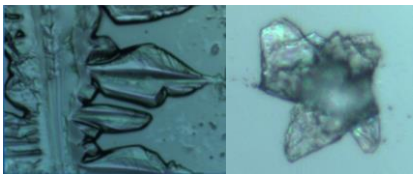

DNA crystals

10 μL of DNA (1μg/μL) in pure water left to dry on a CaF_2 microscope slide

Aikaterini Chatzaki

George Garinis

Human ccfDNA spectral differences in methylation levels

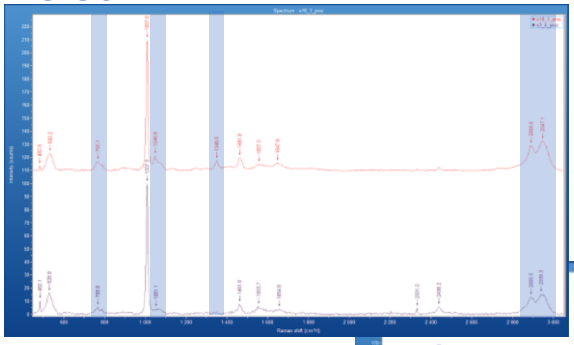

- diabetic
- normal

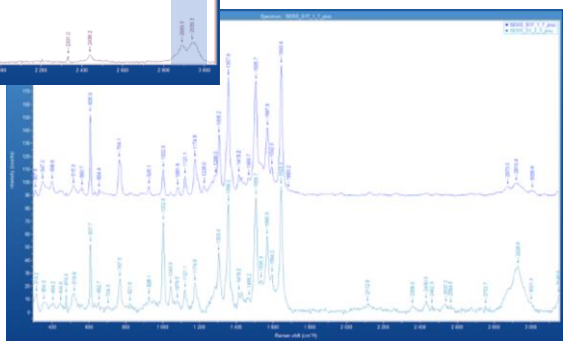

- diabetic
- normal

Human ccfDNA spectral differences in methylation levels

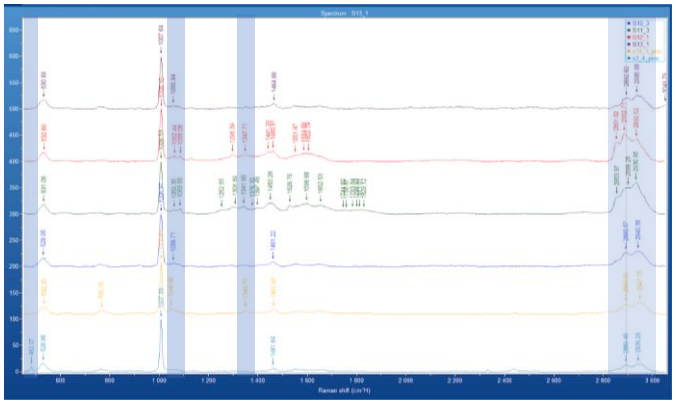

- metastatic
- adjuvant
- adjuvant
- metastatic
- diabetic
- normal

- Major differences appear at 2800 cm^{-1} CH_2/CH_3 region
- Cancer patients present a significant spectral activity in the fingerprint region

Raman spectroscopy characterization of plant DNA methylation levels

- Test methylation levels in WT, KD (RNAi technology) and KO DCL3 (CRISPR technology) plants upon viroid infection
- DNA extracted from *Nicotiana benthamiana* plants

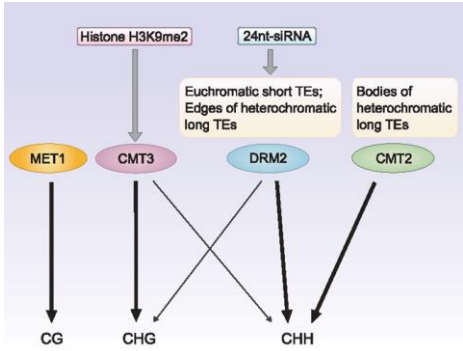


Konstantina Katsarou


Kriton Kalantidis

DNA (*N. benthamiana*) spectral differences in methylation levels

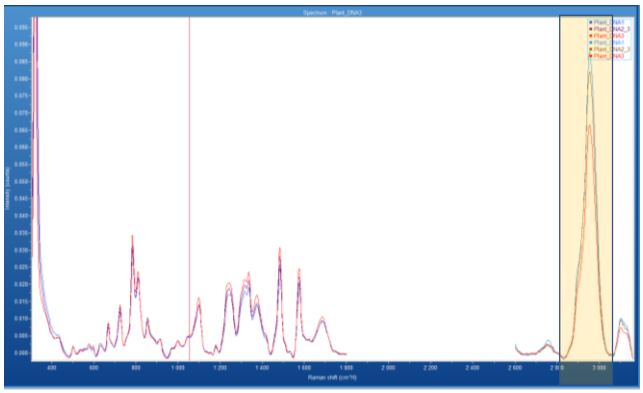

- WT
- KD
- KO

- DNA total methylation is higher in WT plants and is reduced as DICER-LIKE 3 levels decline
- DNA total methylation will be tested in infected and uninfected *N. benthamiana* plants

Cells

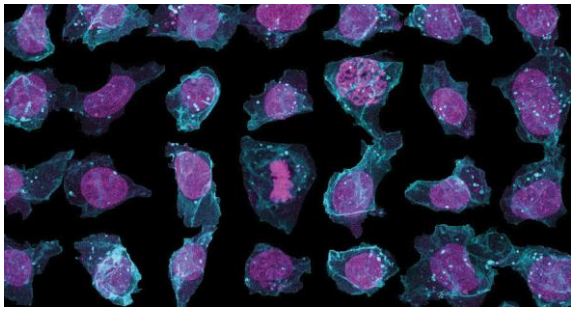

https://www.sciencenews.org/article/allen-cell-explorer-online-portal

Comparison of lymphoma cell types via Raman spectroscopy in order to establish Raman signatures for subtyping or staging

Living cells in phenol-red free medium from 3 lymphoma cell lines: 1 Hodgkin (HL) & 2 Non-Hodgkin (NHL):

MDA-V (HL)
M-1 (NHL)
SUP-M2 (NHL)

Final concentration ➔ 100.000 cells/ml
Final volume in eppendorf ➔ 1ml

20 μl of cell suspension was placed directly on CaF_2 microscope slide

Klytaimnistra Katsara

Konstantina Psatha

Michalis Aivaliotis

Cell-line spectral differences

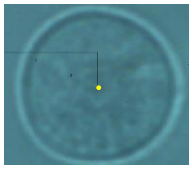

Laser spot size: ~0.7μm
Axial spot size: ~0.8μm
Acquisition time➔ 5 sec
Accumulation number ➔ 3
Distance from the surface ➔ 10-20μm
Time of single measurement ➔ 35 sec

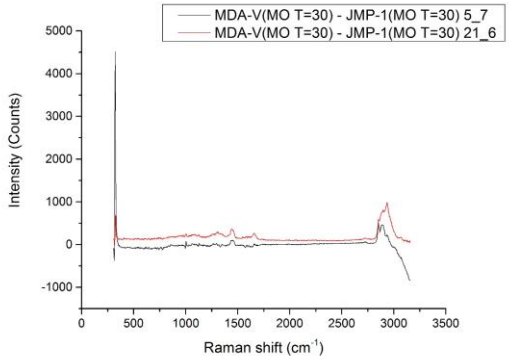

Raman spectral differences derive from averaging of approximately 7 JMP-1 and 3 MDA-V cells
The two colors represent two different experiments under the same conditions

Comparison of lymphoma cell types via Raman spectroscopy after N3a-induced apoptosis in order to study N3a cellular effect

Living cells in phenol-red free medium from 3 lymphoma cell lines +/- N3a; 1 Hodgkin (HL) & 2 Non-Hodgkin (NHL):

MDA-V (HL)
M-1 (NHL)
SUP-M2 (NHL)

Nutlin-3a (N3a): an organic molecule (active enantiomer) of Nutlin-3 racemic mixture, used as a potent therapeutic drug in heamatopoietic malignancies restoring p53 activity

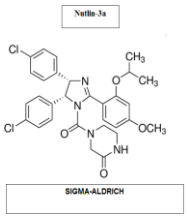


Klytaimnistra Katsara


Konstantina Psatha


Michalis Aivaliotis

N3a Raman reference spectrum

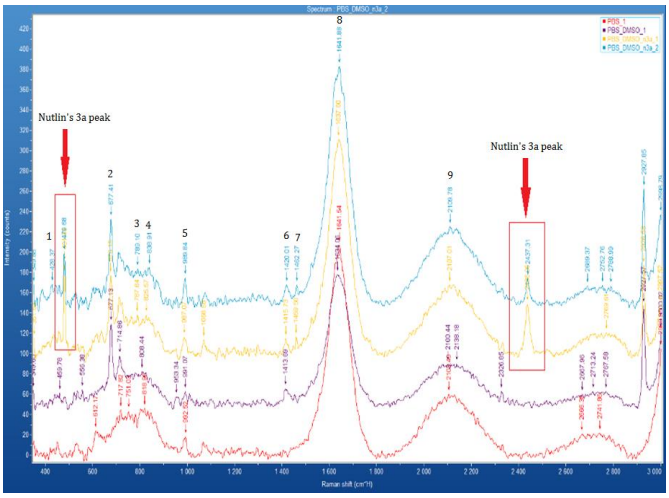

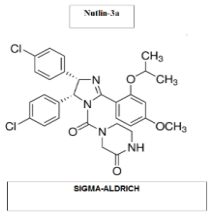

Samples	Unique Raman peaks	Comments
N3a in DMSO and PBS	▪ 2438* ▪ 481 ▪ 1466 (weak)	▪ Raman peaks correspond to N3a.
DMSO in PBS	▪ 700-800 ▪ 2900 ▪ 1400	▪ Raman peaks correspond to DMSO Raman spectral assignments.
PBS (control)	▪ 1600	▪ Raman peaks correspond to PBS Raman spectral assignments.

*not commonly found in biological compounds

▪ N3a ▪ N3a ▪ PBS_DMSO ▪ PBS (control)

Raman spectra of N3a-treated M-1 cells

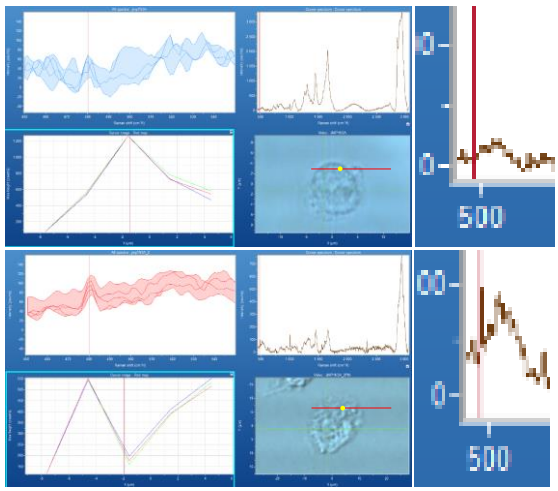

Living cell
No N3a's peaks inside the cell

Lysed cell
N3a's peak is visible inside the cell

Phase separation

- Living/fixed T-cells from mouse (WT, *Satb1* cKO)
- Agent used: w/wo Hexanediol
  (chemical probe used to investigate the material properties of membrane-less nuclear compartments)

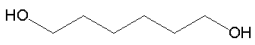

Molecular Formula: $C_6H_{14}O_2$
Molecular Weight: 118.176 g/mol
www.chemisynthesis.com


Tomas Zelenka


Charalambos Spilianakis

Phase separation

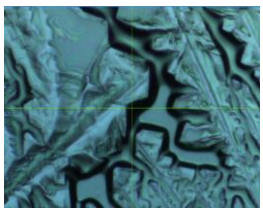

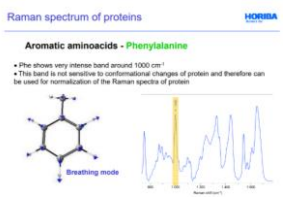

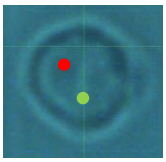

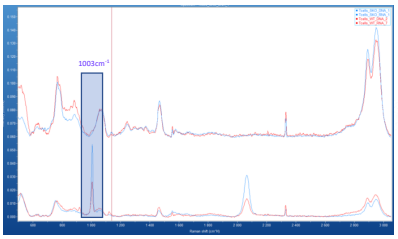

RNA/DNA reference spectra

Nucleus map based on specific Raman peaks

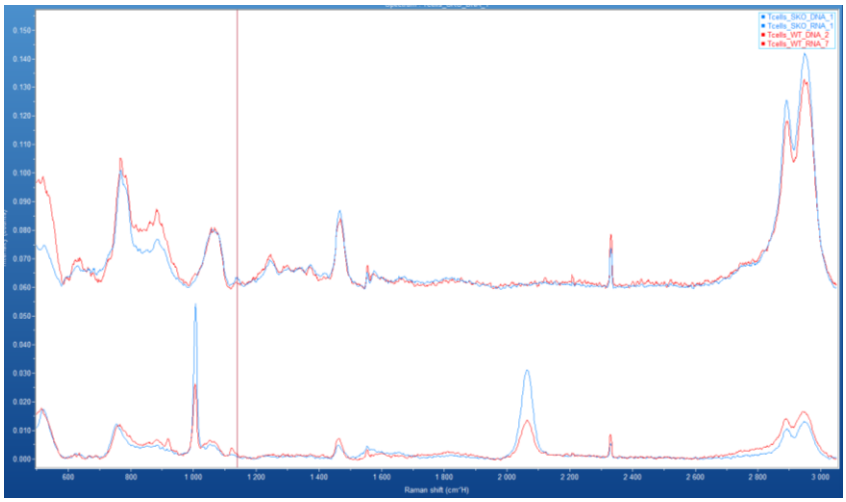

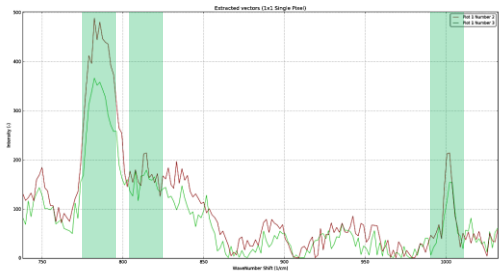

> DNA/RNA (785)

> RNA (813)

> phenylalanine (1004)

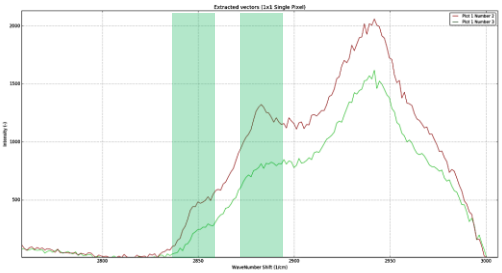

> loosely packed lipids in gauche conformation (2850)

> trans conformation of methyl groups – tightly packed ordered lipids (2870-80)

Raman spectroscopy characterization of plasma membrane lipid changes due to cholesterol depletion

Primary macrophages (fixed)

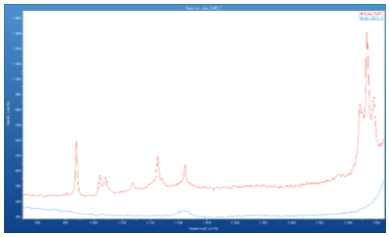

Treatment Raman reference spectum

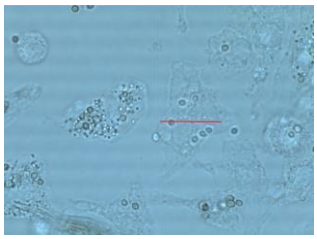

Membrane lipids on macrophages and phagosomes

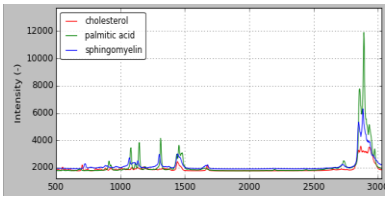

Lipids Raman reference spectrum

Irene Kirmizi

Georgios Hamilos

Macrophage plasma membrane spectral changes after cholesterol depletion

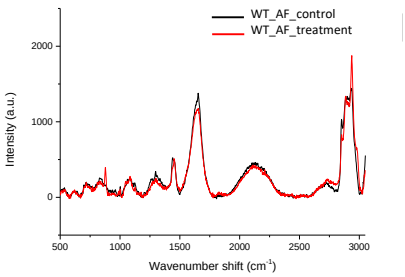

Average spectra from macrophage plasma membrane

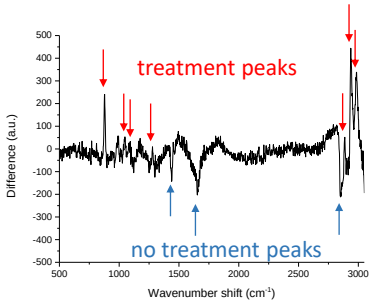

Spectral differences from the average spectra

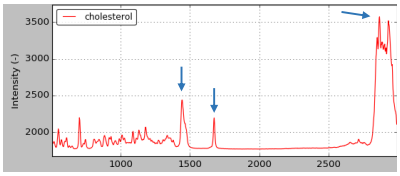

1450: CH_2 bending

1650: amide (a-helix)

2850: CH2 symmetric stretch of lipids

Tissue

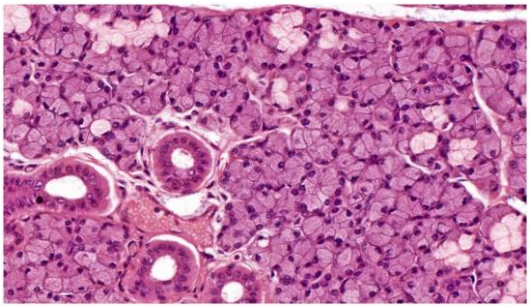

http://www.justscience.in/articles/tissues-in-the-human-body/2017/06/06

Lymphocyte migration in cancerous tissues

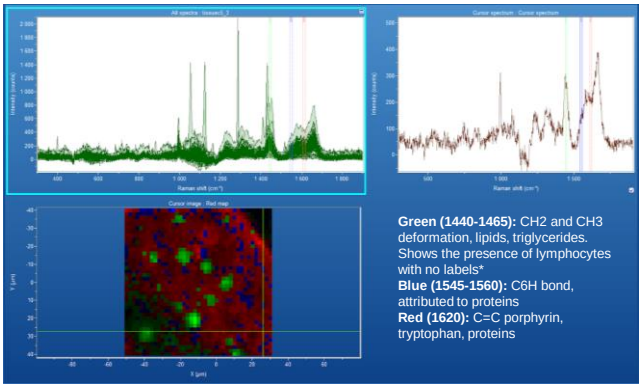

- Deparaffinized tissue mapping
- 25 hour measurement
- Lymphocyte pattern is similar to the map from CD3/CD33 staining

Jason Tasoulas

Stamatios Theocharis

** Mavarani L. et al.. (2013). Spectral histopathology of colon cancer tissue sections by Raman imaging with 532 nm excitation provides label free annotation of lymphocytes, erythrocytes and proliferating nuclei of cancer cells. Analyst 138: 4035-4039*

Mouse liver tissue characterization through novel Raman spectral imaging approaches

Liver tissues

a. normal

b. malignant

Signal Processing

- Principal component analysis (PCA)
- Robust PCA
- Clusterization methods


Grigorios Tsagkatakis


Callina Stratigi


Georgia Chatzinikolaou


George Garinis

Principal Component Analysis (PCA)

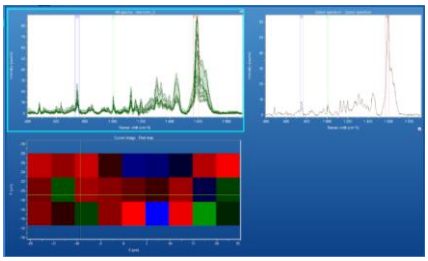

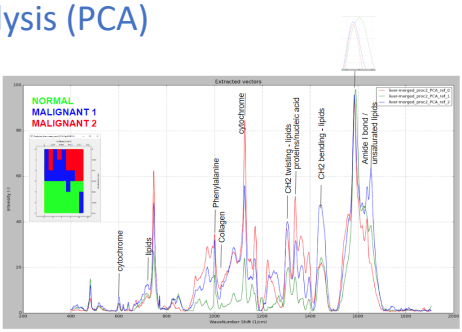

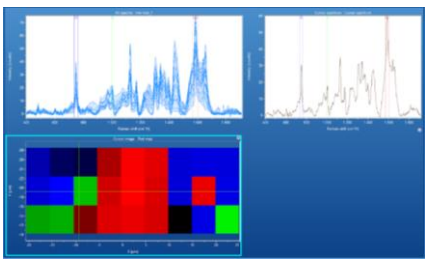

- a wavelength shift is presented around 1580cm^{-1} in both malignant clusters probably due to strain

Robust Principal Component Analysis

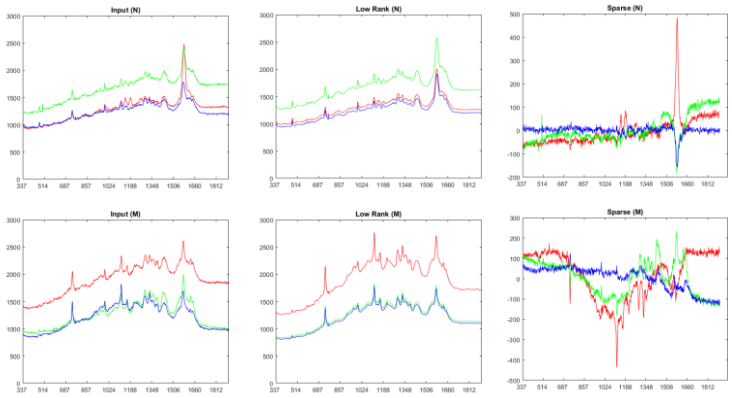

robust PCA results to two spectral curves:

> low rank represents the common spectral features in the whole area map

> sparse signal shows the spectral differences across the area map

Investigation of plastic micro- and nanoparticles uptake by plant roots via Raman spectroscopy

N. benthamiana root sections

Polymer used: polyethylene (plastic water bottle)

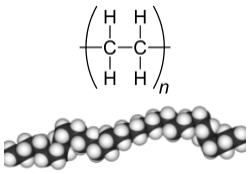

https://en.wikipedia.org/wiki/Polyethylene

Glukeria Mermigka

Panagiotis Sarris

Investigation of plastic micro- and nanoparticles uptake by plant roots via Raman spectroscopy

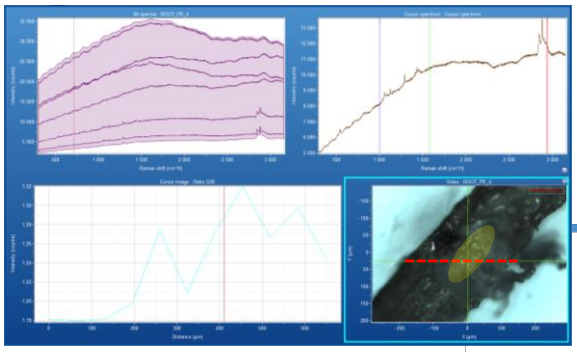

- root signal
- PE reference

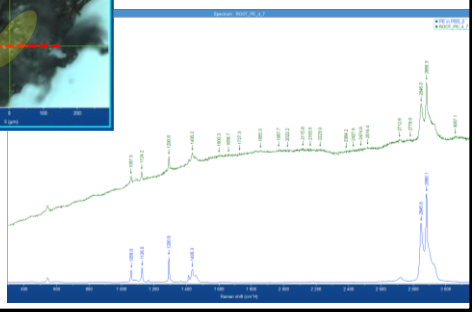

--- line scan across root section

PE cluster

Mouse tissue characterization (subtyping) via Raman spectroscopy

WT mice cryosections (10μm) x54

Tissue	Age	Gender
Liver	37 days	M
Kidney	2 month	F
Muscle	5 month	
	7 month	

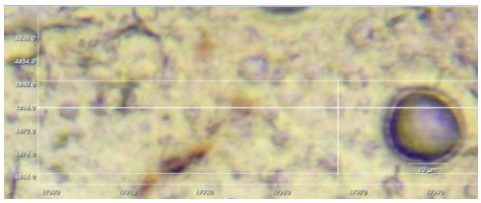

Mouse liver tissue (OB)

<u>Measurement</u>
Size: 150x25μm
Spot size: 1μm
Measurement time: 1h
Substrate: metallic mirror

<u>Signal Processing</u>
> Robust PCA
> Deep learning
> Clusterization methods

Grigorios Tsagkatakis

Ioannis Talianidis

Mouse tissue characterization (phenylalanine map)

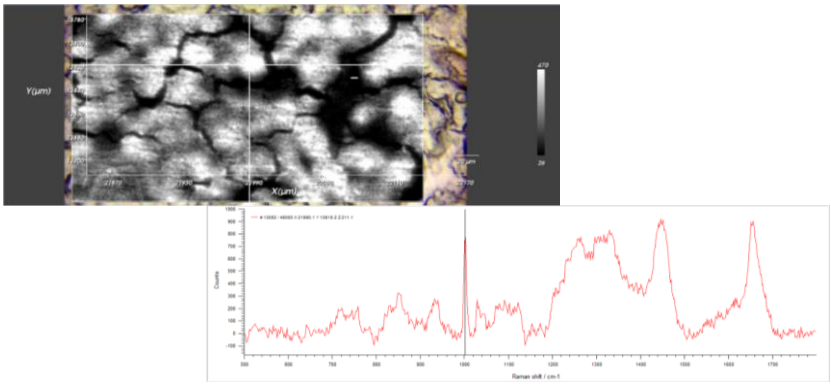

> full spectrum of a point on the liver

> phenylalanine Raman line map on liver tissue

> 3750 total spectra per image map

Mouse tissue characterization (lipids saturation)

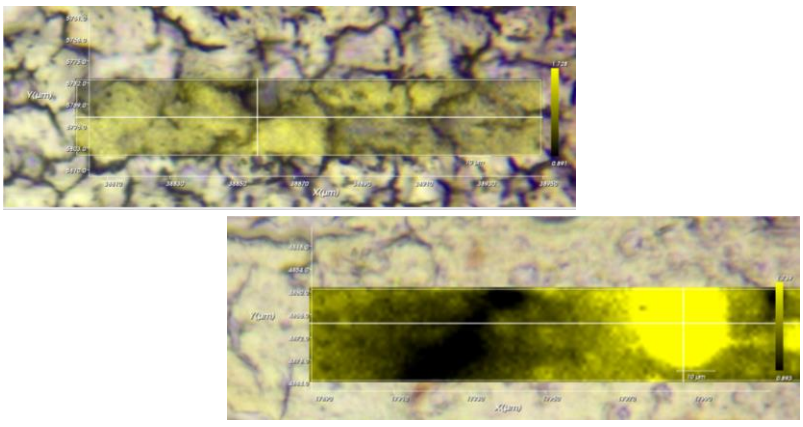

> lipids mapping

> top image: lipid saturation on a normal sample

> lower image: measurement from an OB sample

Plant Stresses characterization (PANTHEON project)

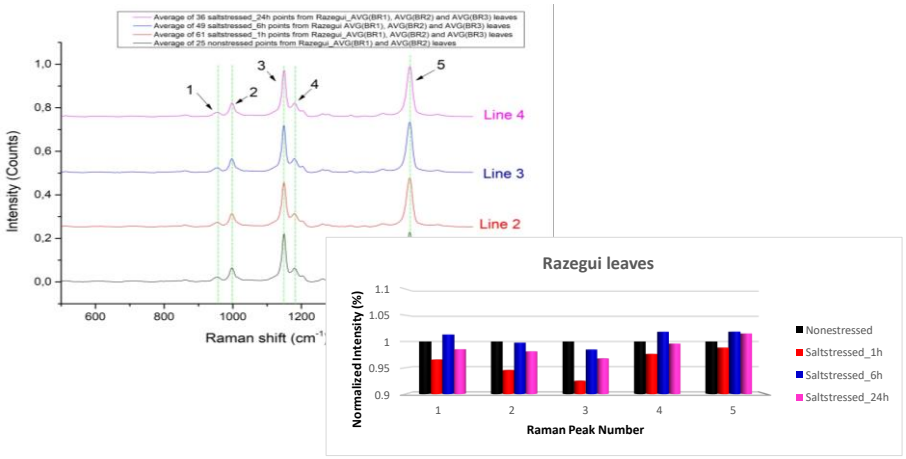

Thank you for your attention!

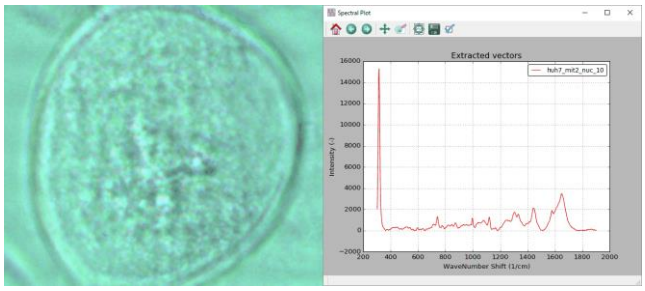

Live-cell Raman spectroscopy

FORTH

ΙΣΝ/SNF ΙΔΡΥΜΑ ΣΤΑΥΡΟΣ ΝΙΑΡΧΟΣ
STAVROS NIARCHOS FOUNDATION